



Blow up in a periodic semilinear heat equation

M. Fasondini^{a,*}, J.R. King^b, J.A.C. Weideman^c

^a School of Computing and Mathematical Sciences, University of Leicester, LE1 7RH Leicester, United Kingdom

^b School of Mathematical Sciences and Synthetic Biology Research Centre, University of Nottingham, NG7 2RD Nottingham, United Kingdom

^c Department of Mathematical Sciences, Stellenbosch University, Stellenbosch 7600, South Africa

ARTICLE INFO

Article history:

Received 30 August 2022

Received in revised form 9 December 2022

Accepted 18 January 2023

Available online 24 January 2023

Communicated by D. Pelinovsky

Keywords:

Nonlinear blow up

Complex singularities

Matched asymptotic expansions

Fourier spectral methods

ABSTRACT

Blow up in a one-dimensional semilinear heat equation is studied using a combination of numerical and analytical tools. The focus is on problems periodic in the space variable and starting out from a nearly flat, positive initial condition. Novel results include asymptotic approximations of the solution on different timescales that are, in combination, valid over the entire space and time interval right up to and including the blow-up time. Both the asymptotic analysis and the numerical methods benefit from a well-known reciprocal substitution that transforms the problem into one that does not blow up but remains bounded. This allows for highly accurate computations of blow-up times and the solution profile at the critical time, which are then used to confirm the asymptotics. The approach also makes it possible to continue a solution numerically beyond the singularity. The specific post-blow-up dynamics are believed to be presented here for the first time.

© 2023 The Author(s). Published by Elsevier B.V. This is an open access article under the CC BY license (<http://creativecommons.org/licenses/by/4.0/>).

1. Introduction

The blow-up phenomenon in nonlinear diffusion equations has been studied extensively in the literature. Some studies focus on physical applications, such as singularity formation in fluids [1–3], runaway in thermal processes [4–6], and biological applications [7]. Others deal with numerical aspects such as the computation of blow-up profiles, estimation of blow-up times, and singularity tracking [8–14]. For general reviews, see [15–17].

The present paper can be viewed as a continuation of [11,14]. The equation considered in these papers is the nonlinear heat equation

$$u_t = u_{xx} + u^2 \quad (1)$$

(although more general nonlinearities and more than one space dimension were also considered in [11]). In this paper we consider the initial condition

$$u(x, 0) = \frac{1}{\alpha - \epsilon \cos x}, \quad 0 < \epsilon \ll \alpha, \quad (2)$$

i.e. periodic, positive and nearly flat with a single maximum on the interval at $x = 0$, leading to a point blow up at $x = 0$, as shown in Fig. 1. This illustrates the well-known strong instability of the spatially uniform solution leading to point blow up. (A broader class of nearly flat initial data that lead to blow up at

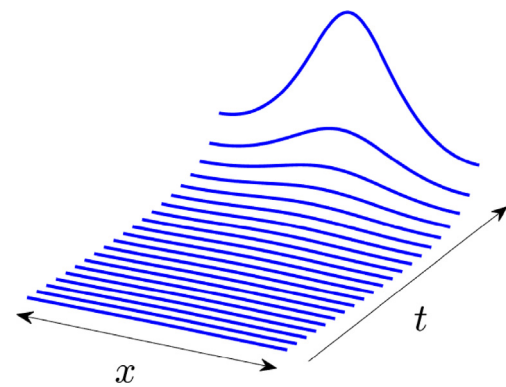


Fig. 1. Typical solution profiles of Eq. (1), in the case of a nearly flat initial condition such as (2). The solution stays almost flat for a long while until a transition to a point blow-up occurs over a relatively short period of time.

the origin is analysed in Appendix A. Initial data with more than one maximum in a period includes the possibility of non-generic blow up, which will be revisited in [18].)

In [14], it was shown by numerical computation that the approach to blow up is not necessarily uniform. That is, there may be times when the diffusive term dominates, leading to a flattening of the solution profile. At other times, particularly near blow up, the nonlinearity dominates, leading to a steepening of the profile. By numerically continuing the solution into the complex plane, it was shown that this behaviour can be associated

* Corresponding author.

E-mail addresses: m.fasondini@leicester.ac.uk (M. Fasondini), John.King@nottingham.ac.uk (J.R. King), weideman@sun.ac.za (J.A.C. Weideman).

with the dynamics of the complex singularities of the solution. When diffusion dominates, they typically move farther from the real axis while the opposite is true when nonlinearity dominates. A point blow up occurs when the singularities reach the real axis. For the nearly flat initial conditions considered in this paper, however, we will show that before the blow-up time is approached there is no simple correspondence between the height of the peak at $x = 0$ and the proximity of the nearest singularity. That is, before the blow-up time, the solution either (depending on the value of α) (i) becomes more steep on $[-\pi, \pi]$ while the singularity is moving away from the real axis or (ii) becomes less steep while the singularity is moving closer to the real axis. Of course, close to the blow-up time, the steepening solution profile is associated with the impingement of singularities onto the real axis at $x = 0$.

In [11], the focus was not on complex singularities but on asymptotic estimation of the blow-up time and the solution profile near blow up. The starting point in that paper was the substitution $u = 1/v$, which transforms (1) into

$$v_t = v_{xx} - 1 - 2(v_x)^2/v. \tag{3}$$

This transformation has advantages for both analysis and computation. Advantages for analysis are spelled out in [4]. For numerical computation, it is easier to deal with solutions tending to zero than to infinity. This avoids the need for specialised rescaling algorithms or moving mesh methods [9,10]. The downside is that the simple polynomial nonlinearity in (1) has been replaced by the more complicated nonlinearity in (3). While this can be ameliorated by multiplication by v , it raises the red flag of division by zero as v becomes small. However, it was shown in [11] and reaffirmed in Section 3 of the present paper that the nonlinear term remains bounded as v approaches zero. This further suggests the possibility of integration through the zero of v , i.e. through the singularity of u , but [11] reported a failed effort. We continued those investigations and announce our findings here.

In [14] periodic boundary conditions were considered while [11] looked at the pure initial value problem on the entire real line. In this paper we continue with the periodic case, as this gives us access to highly accurate Fourier spectral methods (which can also be applied to problems on the infinite line, but with a substantial penalty in accuracy). One contribution here is a conversion of the analysis of [11] to the periodic situation, which is not just a triviality but contributes significant new results as we shall discuss.

For the numerical computations of this paper, a full spectral method based on a Fourier series

$$v(x, t) = \sum_{k=-\infty}^{\infty} c_k(t)e^{ikx}, \quad -\pi \leq x < \pi, \tag{4}$$

was used. The derivatives on the right-hand side of (3) are computed by analytical differentiation of this series, and the nonlinear terms by convolution and de-convolution. The result is an infinite system of ODEs for the evolution of the Fourier coefficients c_k , which gets truncated at $|k| = N$, with $N \gg 1$. The procedure for choosing N was the standard one of increasing its value until the results have converged to the required number of digits (for tabulated values) or to visual accuracy (for figures). In all cases, a value of $N = 128$ was sufficient. We check the validity of our numerical error estimates by comparing it to an estimate of the truncation error derived using our asymptotic approximations.

To integrate the system of ODEs we used ode45, MATLAB's standard ODE solver, as well as ode15s, its stiff solver [19]. The latter solver executes faster for larger N because the system is mildly stiff, but accuracy and not speed was the primary

concern here. The main value of these solvers is the adaptive time stepping that aims to maintain accuracy at a prescribed level. The tolerance parameters for this were set to a stringent 10^{-12} . At these levels the results of ode45 and ode15s were indistinguishable.

In order to compute the time $t = t_c$ at which the numerical solution blows up (i.e. $v = 0$ is attained), we used the fact that the initial conditions considered here lead to blow up at $x = 0$ and hence we check when the sum of the c_k equals zero. Both of the ODE solvers alluded to above can be called with the 'event' option, which offers rootfinding capabilities that allowed us to solve for t_c from $\sum c_k(t) = 0$. The accuracy tolerance for the rootfinding is the same as the set tolerance for the ODE solver.

We use this numerical solution as reference solution for the purposes of checking the various asymptotic estimates. Because of the relatively smooth nature of v , even at the critical time (as will be discussed), we believe it is sufficiently close to the true solution for all verification purposes.

The three main sections of the paper can be summarised in a nutshell as: before blow up, at blow up, and after blow up. More specifically, in Section 2 we present a perturbation analysis that approximates the solution to (3) accurately to $O(\epsilon^2)$ on the entire periodic space domain and the whole time interval until a time that is $O(\epsilon)$ close to blow up. Beyond that time up to the blow-up point it has to be modified and this is done by matched asymptotic expansions, the details of which are contained in Appendix A. In this appendix we also analyse the dynamics of the singularities of the solution and in Appendix B the relation between the proximity of the singularities to the real axis and the steepness of the solution profile on $[-\pi, \pi]$ is clarified. In Sections 2 and 3, the analyses in the appendices are confirmed by numerical experiments. In Appendix C, we derive an estimate of the spatial truncation error of the numerical method that is valid up to the blow-up time. Section 4 is a first report on integrating through the singularity at the blow-up time and the subsequent evolution.

2. Two-mode perturbation analysis

The analysis of [11] was based on the truncated Taylor expansion

$$v \approx a(t) + b(t)x^2. \tag{5}$$

By substituting into (3) and dropping powers of x^4 the problem was reduced to a dynamical system in the variables a and b ; see (18). Here we follow an analogous procedure, but consider instead a truncated Fourier expansion

$$v \approx a(t) - b(t) \cos x. \tag{6}$$

Under the assumption of strictly positive solutions, i.e., $0 < b(t) < a(t)$, both of these approximations blow up (in the variable $u = 1/v$) in finite time at $x = 0$.

Substitution of (6) into (3) and neglecting $\cos 2x$ contributions gives the system

$$a \frac{da}{dt} + \frac{1}{2}b \frac{db}{dt} = -a - \frac{3}{2}b^2, \quad b \frac{da}{dt} + a \frac{db}{dt} = -ab - b, \tag{7}$$

or, in explicit form,

$$\frac{da}{dt} = \frac{2ab^2 + 2a^2 - b^2}{b^2 - 2a^2}, \quad \frac{db}{dt} = \frac{b(2a^2 - 3b^2)}{b^2 - 2a^2}. \tag{8}$$

(Note that the assumption $0 < b < a$ precludes the vanishing of the denominators.) The phase plane of this system is shown in Fig. 2.

Consider solution curves in Fig. 2 that originate near $b = 0$, say

$$a(0) = \alpha, \quad b(0) = \epsilon, \quad 0 < \epsilon \ll \alpha. \tag{9}$$

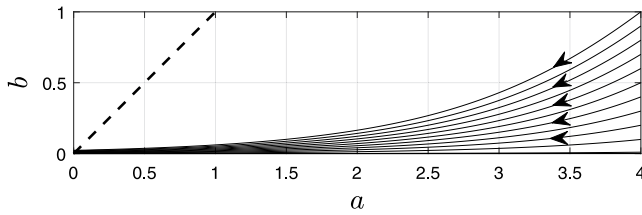


Fig. 2. Phase plane of the system (8) in the domain $0 < b < a$. The analysis of this section approximates solution curves close to $b = 0$. Blow up at $x = 0$ in the u -equation (1) corresponds to solution trajectories intersecting the dashed line $b = a$.

As an explicit solution of the system (7) appears not to exist, we settle for a perturbation analysis, by expanding

$$a = a_0(t) + \epsilon a_1(t) + O(\epsilon^2), \quad b = \epsilon b_1(t) + O(\epsilon^2) \tag{10}$$

where $a_0(0) = \alpha$, $b_1(0) = 1$, $a_1(0) = 0$. Substitution into (7) gives, to zeroth order

$$a_0 \frac{da_0}{dt} = -a_0 \Rightarrow a_0 = \alpha - t. \tag{11}$$

At $O(\epsilon)$,

$$\frac{da_1}{dt} = 0, \quad \frac{db_1}{dt} = -b_1 \Rightarrow a_1 = 0, \quad b_1 = e^{-t}. \tag{12}$$

This gives, to $O(\epsilon^2)$, the approximate solution

$$\tilde{v} = \alpha - t - \epsilon e^{-t} \cos x. \tag{13}$$

Plugging this expression into (3) gives

$$\tilde{v}(\tilde{v}_t - \tilde{v}_{xx} + 1 + 2(\tilde{v}_x)^2/\tilde{v}) = 2\epsilon^2 e^{-2t} \sin^2 x, \tag{14}$$

which confirms that the v -equation is satisfied to $O(\epsilon^2)$ uniformly in x , for all \tilde{v} bounded away from zero. Fig. 3 illustrates that the perturbation approximation (13) and the (numerically computed) solution to the two-mode system (8) are good approximations to the numerical reference solution of (3) on most of the interval $[0, t_c)$, where t_c is the critical time at which blow up occurs. As $t \rightarrow t_c$, the assumption underlying the perturbation analysis and the two-mode approximation, $b(t) \ll a(t)$, is no longer valid, however, and the approximations lose accuracy, an issue that we address in Appendix A.

Various estimates can be obtained from the perturbation solution (13). By setting $\tilde{v} = 0$ at $x = 0$ and excluding $O(\epsilon^2)$ terms, for example, one obtains the following estimate for the blow-up time

$$t_c \approx \hat{t}_c := \alpha - e^{-\alpha} \epsilon. \tag{15}$$

In Appendix A, using the method of matched asymptotic expansions, a higher-order estimate of t_c is derived (see (43) and (67)):

$$t_c \approx \tilde{t}_c := \alpha - e^{-\alpha} \epsilon - (2C_1 + C_2 + C_3)\epsilon^2, \tag{16}$$

the constants C_i being defined in (66). The accuracy of these estimates is verified in Table 1. (The values of t_c listed in the table were computed by the method described in Section 1, and are believed to be correct to all digits shown.)

The singularity dynamics mentioned in the introduction can be estimated as follows. The complex singularity in the u -equation corresponds to a complex zero of the v -equation. This is located at $x = iy$ with y real, and setting $\tilde{v} = 0$ gives

$$y = \cosh^{-1}((\alpha - t)e^t/\epsilon). \tag{17}$$

For reasons implicit in the analysis of Appendix A, this approximation is valid, however, only for small values of y , i.e., near (but not too near) blow up. This follows from the fact that the

Table 1

Blow-up times for various parameter choices in the initial condition (2): t_c is the blow-up time as computed from the reference solution, t'_c is the blow-up time as estimated from a numerical solution of the two-mode system (7) and \hat{t}_c and \tilde{t}_c denote the estimates (15) and (16), respectively.

ϵ	$\alpha = 0.25$			
	t_c	$t'_c - t_c$	$\hat{t}_c - t_c$	$\tilde{t}_c - t_c$
0.1	0.161963	-3.6e-04	1.0e-02	2.6e-02
0.01	0.242093	1.8e-03	1.2e-04	2.8e-04
0.001	0.249220	2.2e-04	1.2e-06	2.8e-06
$\alpha = 1$				
0.1	0.955542	2.1e-03	7.7e-03	4.5e-03
0.01	0.996241	9.5e-04	8.1e-05	4.9e-05
0.001	0.999631	1.1e-04	8.1e-07	4.9e-07
$\alpha = 4$				
0.1	3.996685	5.0e-04	1.5e-03	1.4e-05
0.01	3.999802	5.3e-05	1.5e-05	1.2e-07
0.001	3.999982	5.4e-06	1.5e-07	1.2e-09

remainder term on the right-hand side of (14) grows exponentially with y . In Fig. 4, the asymptotic estimate (17) is compared to a numerical estimate of the singularity location obtained via the method of [12], which is essentially an estimation of the width of the strip of analyticity of the solution, by examining the rate of decay of its Fourier coefficients. To apply the method of [12], we use the fact that, to leading order and away from the blow-up time, singularities of solutions to the u -equation are second-order poles.¹ Fig. 4 also shows asymptotic estimates of the singularity location that are derived in Appendix A.4 by the method of matched asymptotic expansions. The estimates are valid in the limits $t \rightarrow 0^+$ and $t \rightarrow t_c^-$ but in between, for $t = O(1)$, the singularity location of the original PDE (3) is described by the singularity location of a more difficult nonlinear initial value problem (68)–(70) which is not analytically solvable. The asymptotics nonetheless correctly indicate the initial movement of the singularity away from the real axis (at a speed that becomes infinite as $t \rightarrow 0^+$) and the final motion shortly before the singularity collides with the real axis at $t = t_c$.

In Appendix B we investigate the relationship between the position of the complex singularity and the height of the peak of the solution profile in the u -variable (which is located at $x = 0$; see Fig. 1) relative to the solution value at $x = \pm\pi$.

Returning to the analysis of [11], which was based on the truncated Taylor approximation (5), we note that the focus in that paper was on the behaviour at $t = t_c$, not the evolution on $[0, t_c)$ as is the focus in this section. It is therefore instructive to adapt that analysis here and compare results to (13) and (14).

The dynamical system analogous to (7)–(8) is now

$$\frac{da}{dt} = 2b - 1, \quad a \frac{db}{dt} = -8b^2. \tag{18}$$

This is a much simpler system, and in fact admits a first integral $2 \log b + 1/b + b \log a = \text{constant}$, although we shall not make use of this result and neither was it used in [11]. (No such first integral could be found for (7)–(8).)

Proceeding with a perturbation analysis based on (9)–(10) give $a_0 = \alpha - t$, $a_1(t) = 2$, and $b_1(t) = 1$. Therefore, excluding $O(\epsilon^2)$

¹ In [18] we show that these singularities are in fact logarithmic branch points, however the branch point singularity appears in the fourth-order term in the local expansion about the singularity. Therefore, for the purpose of estimating the position of the singularity, we only use its leading-order, second-order pole behaviour. We shall find in Section 3 that in the limit $t \rightarrow t_c$, the leading order behaviour of the singularity at $x = 0$, which results from the coalescence of two singularities, is of a more complicated form than that of a second-order pole.

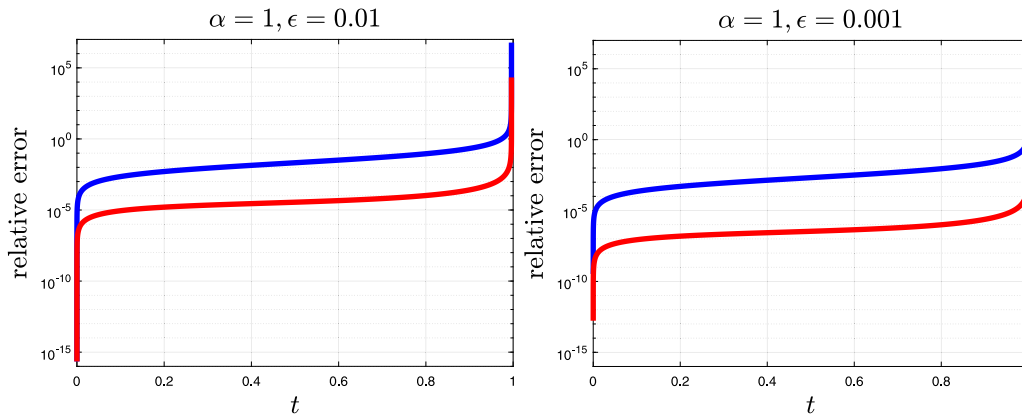


Fig. 3. The maximum relative error on $[-\pi, \pi]$ of the perturbation approximation (13) (blue) and the numerical solution to the two-mode system (8) (red) as a function of t . The errors are calculated with reference to the numerical solution of (3) described in Section 1.

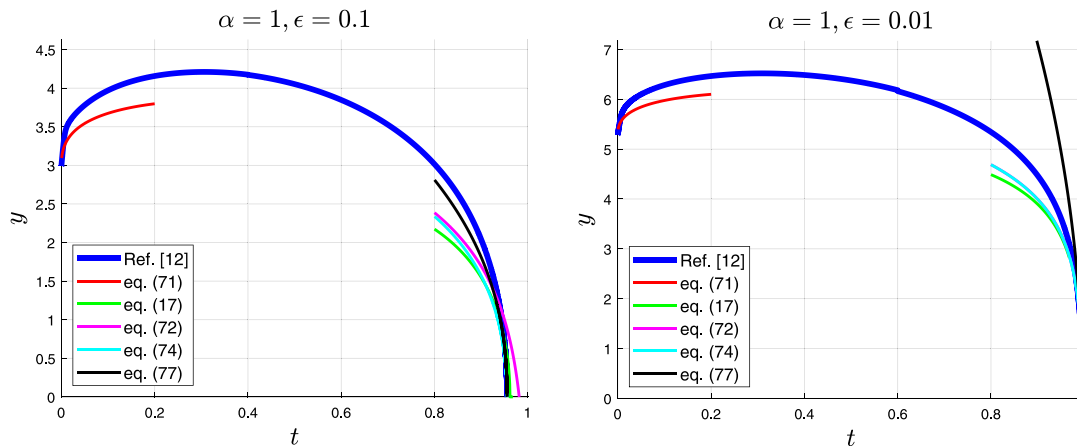


Fig. 4. The position on the positive imaginary axis of the singularity of the solution to (3) with initial condition $v(x, 0) = \alpha - \epsilon \cos x$. (In the right frame, the approximation (72) is not visible because it is indistinguishable from (74).)

terms, v is approximately

$$\tilde{v} = \alpha - t + \epsilon(2t + x^2) \tag{19}$$

in analogy with (13). Plugging into (3) gives

$$\tilde{v}(\tilde{v}_t - \tilde{v}_{xx} + 1 + 2(\tilde{v}_x)^2/\tilde{v}) = 8\epsilon^2 x^2. \tag{20}$$

Comparing with (14) shows an advantage of the periodic analysis, namely that its right-hand side is $O(\epsilon^2)$ uniformly in x , whereas the right-hand side of (20) is $O(\epsilon^2)$ only if $x^2 = O(1)$. That is, with \tilde{v} bounded away from zero (13) can provide a valid approximation over the entire (periodic) domain, while (19) is valid only near $x = 0$. On the other hand, the advantage of the analysis of [11] is that it gives a valid description of the structure of the solution close to blow up, as discussed in Appendix A.

3. Solution in the blow-up limit

Appendix A is devoted to an asymptotic analysis of the solution on three time scales (labelled (I), (II) and (III) in the appendix) that are progressively closer to the blow-up time, namely $t = O(1)$, $T = (t - t_c)/\epsilon = O(1)$ and $\tau = -\epsilon \log(-T) = -\epsilon \log((t_c - t)/\epsilon) = O(1)$. The analysis is performed using the method of matched asymptotics and the results on the first time scale are the same as the those obtained in Section 2 via a regular perturbation analysis (in particular, recall the approximation (13) and its failure close to the blow-up time, as seen in Fig. 3).

On the second time scale, $T = O(1)$, the following asymptotic approximation is derived for $x = O(1)$:

$$\begin{aligned} v \sim & t_c - t + 2\epsilon e^{-\alpha} \sin^2(x/2) \\ & + 2\epsilon^2 \log \epsilon e^{-2\alpha} \sin^2 x + \epsilon(t - t_c)e^{-\alpha} \cos x \\ & + 2\epsilon^2 \sin^2 x \left(e^{-2\alpha} \log \left(\frac{t_c - t}{\epsilon} + 2e^{-\alpha} \sin^2(x/2) \right) + C_1 + C_3 \right), \end{aligned} \tag{21}$$

which is obtained by combining (44)–(46) and (65)–(67). As shown in Appendix A.3, we can set $t = t_c$ in (21) to obtain a representation of the solution that is valid on the third time scale for $x = O(1)$, noting that $\tau = O(1)$ corresponds to t being exponentially close to t_c . Thus, as $t \rightarrow t_c^-$, $\epsilon \rightarrow 0$ with $x = O(1)$, we have

$$\begin{aligned} v \sim & 2\epsilon e^{-\alpha} \sin^2(x/2) \\ & + 2\epsilon^2 \sin^2 x \left(e^{-2\alpha} \log (2\epsilon e^{-\alpha} \sin^2(x/2)) + C_1 + C_3 \right). \end{aligned} \tag{22}$$

Fig. 5 verifies the accuracy of the asymptotic approximations (13) (away from the blow-up time) and (21)–(22) (close to and at the blow-up time). The left frame of Fig. 6 shows the numerical solution at the blow-up time with the blow-up profile (22) superimposed on it. Hence, we have accurate asymptotic expressions for the solution on the entire spatial interval $x \in [-\pi, \pi]$ and from $t = 0$ all the way up to and including the blow-up time. For $x \rightarrow 0$ at $t = t_c$, however, we shall need another asymptotic approximation, namely (24), to be discussed below.

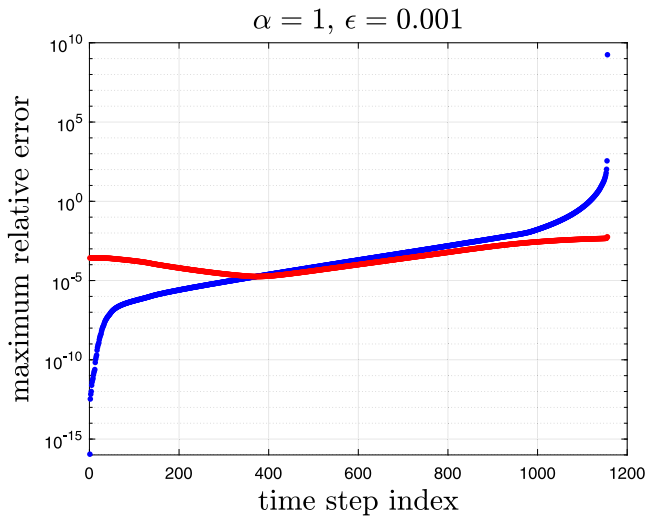


Fig. 5. Errors in the asymptotic approximations (13) (blue) and (21) (red) when compared to the reference solution. The ODE solver returns approximations at times $t = t_k$, $k = 0, 1, \dots, M$, where $t_0 = 0$ and $t_M = t_c$. Here $M = 1155$ and $t_c = 0.9996$ (more digits are listed in Table 1). At each $t = t_k$, the maximum relative errors of (13) and (21) are calculated on the interval $x \in [-\pi, \pi]$ and plotted against the time step index k . Because of the adaptive time-stepping, the t_k values are not equidistant, but the spacing is much denser near $t = t_c$. As an indication of this, note that the two curves intersect at $k = 372$ and $t_{372} \approx 0.973$, which is already quite close to the critical time t_c even though roughly 800 more time steps are to be taken. From the asymptotic analysis, we expect the approximation on the first time scale (13) (blue) to start to break down and (21) (red) to be valid on the second time scale when $(t_c - t)/\epsilon = O(1)$. Here we have that at around $k = 800$, $t_c - t_k \approx \epsilon = 0.001$, which is indeed when the error curves of the two approximations start to diverge noticeably.

The rate of decay of the Fourier coefficients of v will be of relevance in the next section when we consider the possibility of continuing the solution beyond blow-up. From (22) we deduce that the c_k decay as $O(k^{-3})$ close to the blow-up time because

$$\frac{1}{2\pi} \int_{-\pi}^{\pi} \sin^2 x \log(\sin^2(x/2)) e^{-ikx} dx = \frac{2}{k(k^2 - 4)}$$

which implies that

$$c_k(t_c) \sim \frac{4\epsilon^2 e^{-2\alpha}}{k^3}, \quad k \rightarrow \infty. \tag{23}$$

The right frame of Fig. 6 confirms the accuracy of this estimate as $\epsilon \rightarrow 0$.

At the blow-up time, for x exponentially small with respect to ϵ , (22) is no longer valid (see the discussion below (61)). Instead,

$$v \sim \frac{\epsilon e^{-\alpha x^2}}{2 - 8\epsilon e^{-\alpha} \log(x^2)} \sim -\frac{x^2}{16 \log|x|}, \tag{24}$$

which follows from (62) and (67). Fig. 7 confirms that (24) has better accuracy than (22) for small x at the blow-up time.

Regarding the strength of the singularity at $x = 0$, it follows from (24) that $v^{(n)} \rightarrow 0$ as $x \rightarrow 0$ for $n = 0, 1, 2$ but the third derivative blows up as $v^{(3)} = O\left(\frac{1}{x \log^2|x|}\right)$, $x \rightarrow 0$. A singularity with two bounded derivatives is consistent with the $O(k^{-3})$ decay of the Fourier coefficients that was derived from (22).³ In fact, the asymptotic approximation (24) suggests that the

² Ideally, we would show the accuracy of (24) for even smaller values of x than those in Fig. 7. However, this would require high-precision computations. In standard double precision (with a machine precision of approximately 10^{-16}) we cannot compute the errors for smaller x because round-off errors prevent the accurate evaluation of v from its numerically computed Fourier coefficients.

³ The ‘global’ blow-up profile (22) has a stronger singularity at $x = 0$ than the ‘local’ blow-up profile (24) since the second derivative of the former blows

Fourier coefficients of the solution precisely at the blow-up time decay slightly faster than the $O(k^{-3})$ suggested by (23). To show this, symmetry and integration by parts can be used to obtain

$$c_k(t_c) = \frac{1}{\pi} \int_0^{\pi} v \cos kx = \frac{1}{\pi k^3} \int_0^{\pi} v''' \sin kx dx.$$

From (24) it follows that $v \sim -x^2/(8 \log(x^2))$, $v''' \sim 1/(8x \log^2(x))$, and by making the change of variable $x = \mu/k$ with $k \gg \mu$, one obtains,

$$c_k(t_c) \sim \frac{1}{8\pi k^3 \log^2 k} \int_0^{\infty} \frac{\sin \mu}{\mu} d\mu = \frac{1}{16k^3 \log^2 k}. \tag{25}$$

The solid line in Fig. 6 shows the estimate (25), which, unlike the estimate (23), is independent of ϵ and α . The numerical Fourier coefficients shown in Fig. 7 do not decay as fast as (25), which suggests that one would need to perform computations of extremely high precision to observe the rate of decay predicted by (25).

For the possible continuation beyond blow-up one needs to confirm that the nonlinear term in the v -equation (3), i.e., $(v_x)^2/v$, remains bounded at $x = 0$ at the blow-up time. In fact, from (24) it follows that the nonlinear term vanishes, according to $O(1/\log|x|)$, for $x \rightarrow 0$.

4. Integrating through the singularity

The fact that the nonlinear term in (3) remains bounded as v approaches zero raises the intriguing possibility of numerically integrating through the blow up. This was tried in [11], but the authors found “...the calculation actually continues the solution slightly beyond the blow-up time of the original solution u . The method becomes unstable a short time after the blow-up happens, however”. We report here on renewed efforts in this direction. (Details of how our numerical strategies differ from those of [11] are postponed to the end of the section.)

Fig. 8 shows a series of snapshots of the solution v at different times. First, observe that there is no sign of instability as the solution passes smoothly through $v = 0$ (third frame). What happens next might be unexpected, namely, the solution turns complex, which is consistent with the fact that real solutions cannot be continued past blow up [16]. In addition, uniqueness is lost: By experimenting with different variations of our numerical methods (discussed below) we have observed a total of four solutions post blow-up. The four are represented in Fig. 10. Surprising as these results may be, both the non-uniqueness and the fact that the solution turns complex are consistent with theoretical results of [20].

Fig. 9 shows the u -solution that corresponds to the v -solution in Fig. 8. After the solution turns complex at the critical time (third frame) the modulus of u shows wave-like behaviour, with two waves travelling in opposite directions from the origin until they reach the edge of the domain $x = \pm\pi$. Because of periodicity they meet up with similar waves from adjacent intervals and a second blow up almost occurs, this time at $x = \pm\pi$ (seventh frame). The modulus grows considerably and we conjecture that by varying the parameters in the initial condition a proper secondary blow up may be found. Computing over a longer time interval suggests that u asymptotically approaches the constant (and real) solution $u \sim -1/t$ as $t \rightarrow \infty$.

We present the results of Figs. 8 and 9 knowing full well that we have little theory to present as validation. The theoretical results of [20] suggest the possibility of a complex and non-unique

up logarithmically at $x = 0$, while for the local profile $v^{(2)} \sim 0$ as $x \rightarrow 0$. The Fourier coefficients of the ‘global’ profile nevertheless decay at the correct $O(k^{-3})$ rate since its second derivative, though unbounded, is integrable.

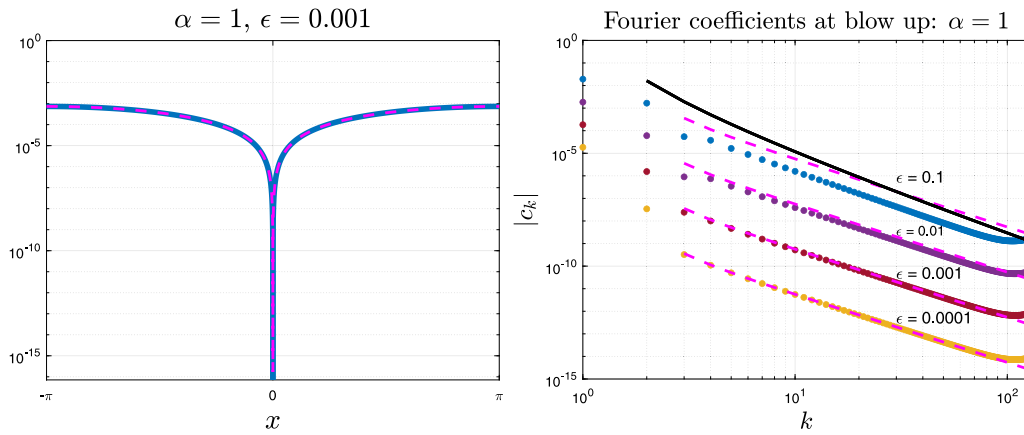


Fig. 6. Left: The solution to the v -equation (3), displayed on a semi-log-scale, at the blow-up time t_c (solid curve) compared to the asymptotic estimate (22) (dashed curve on top of the solid curve; the relative error of this approximation is shown in the right frame of Fig. 7). Here we would like to draw attention to the fact that, at the origin and at the critical time, the values of v are computed to levels close to roundoff error ($\sim 10^{-16}$), which translates into huge values in the u solution near blow up. (See for example the third frame in Fig. 9.) This is a consequence of solving equation (3) instead of (1). Right: The Fourier coefficients of the reference numerical solution at the blow-up time (dots) compared to the coefficients of the global asymptotic blow-up profile (dashed lines), given in (23). The single solid line shows the asymptotic estimate of the decay of the Fourier coefficients of the local blow-up profile (see (25)).

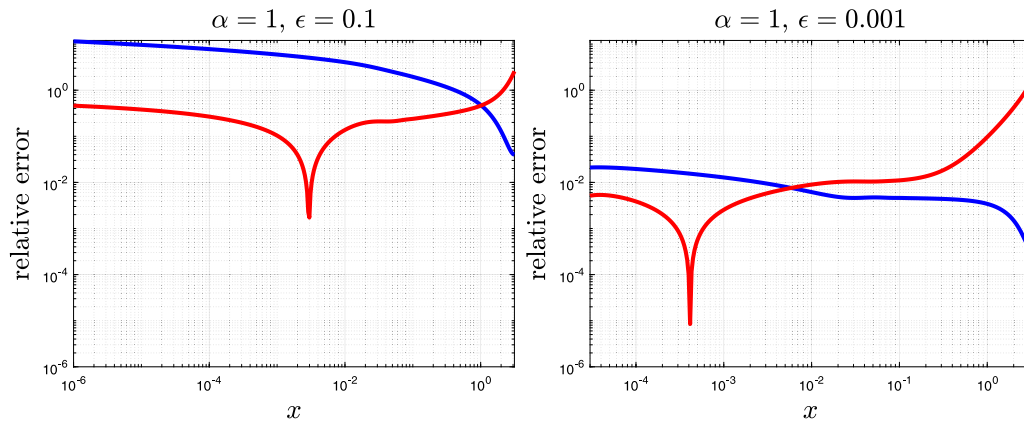


Fig. 7. The relative error of the asymptotic approximations (22) (blue) and (24) (red) at the blow-up time for small x .

solution post blow-up, but does not allow for a quantitative comparison. Nevertheless, the following heuristic observations support the validity of the results shown here.

Firstly, the fact that the numerical solution approaches $-1/t$ as $t \rightarrow \infty$ provides some confidence, as this solves (1) exactly. Secondly, as noted before, the singularity in the v -equation at the critical time is rather weak, leading to Fourier coefficients that decay at the relatively rapid rate $c_k = O(1/(k^3 \log^2 k))$; recall (25). While still much slower than the typical exponential decay rate for analytic periodic functions, we conjecture that this decay is nevertheless sufficiently rapid that the accuracy loss of the spectral method at the critical time is not disastrous. Fig. 11 shows the Fourier coefficients near and at the critical time.

To get a quantitative sense of the accuracy of the numerical solution at the critical time, we note that the results displayed in Figs. 8 and 9 were computed with $2N + 1$ terms in the approximation series (4), with $N = 128$. When the number of terms was increased to $4N + 1$, the relative difference in the two v -solutions, as measured in the 2-norm on $[-\pi, \pi]$, was approximately 6×10^{-7} . This agrees to within an order of magnitude with the relative error estimate (82) derived in Appendix C, which for the parameter values in Figs. 8 and 9 is 3×10^{-7} . This suggests that the displayed solution at the critical time has converged to about six or seven significant decimal digits.

To the best of our knowledge, the only published results that deal with numerical computations of post-blow-up solutions

are [21,22]. These authors based their computations on complexification of the t -variable. Following this idea we integrated along a path that contains a semi-circle in the complex t -plane, centred at the estimated singularity. Using this approach we obtained results to within 10^{-8} of those of Fig. 9 (after the critical time), which lends further credibility to the results shown here.

It should be noted that the authors of [21,22] based their methods on the u -equation, not the v -equation. Because u grows without bound near the critical time, these methods cannot compute blow-up solutions in the immediate neighbourhood of the critical time accurately. For the same reason, estimates of blow-up times are unreliable. Adapting these methods from the u -equation to the v -equation should not be hard to do, however.

The observation of a complex solution after the critical time has lead us to conjecture that the failure of the finite-difference method of [11] was because it was almost surely coded as a real system using real arithmetic. To allow for the possibility of a complex solution we have explored the following two strategies.

The first was to use the complex form of the Fourier series (4) (rather than the real form). In a software system such as MATLAB that uses complex floating-point arithmetic by default, this introduces an imaginary component at the level of roundoff error. The second was to split the v -equation (3) into its real and imaginary parts, and integrate this as a real, coupled system. In this case the imaginary component was introduced manually

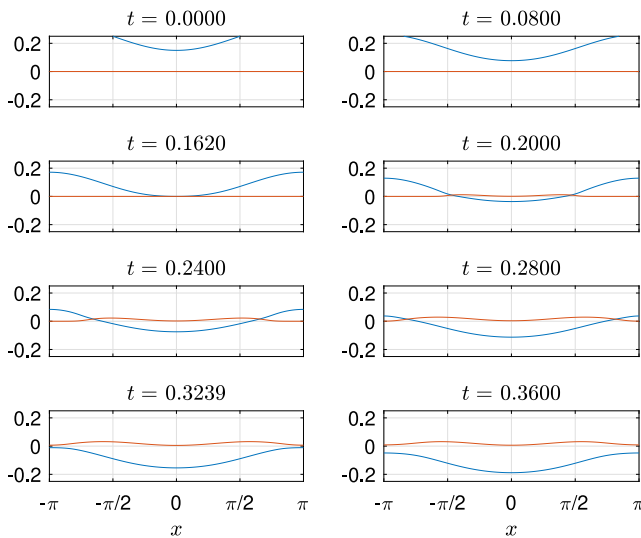


Fig. 8. Solution to the v -equation (3) corresponding to the initial condition (2) with $\alpha = 0.25$, $\epsilon = 0.1$. (The corresponding u solution is shown in Fig. 9, and a movie of the dynamics can be seen in the supplementary material that accompanies this paper.) The two noteworthy times are $t = t_c$ (third frame) and $t = 2t_c$ (seventh frame), where $t_c = 0.162$, approximately. At $t = t_c$ there is a zero of v at $x = 0$, after which the solution turns complex: the real part is shown in blue and the imaginary part in red. At $t = 2t_c$ there are approximate zeros of v near $x = \pm\pi$. The solution shown is not unique (see Fig. 10). Changing the values of α and ϵ to the other values listed in Table 1 gives pictures that are qualitatively similar.

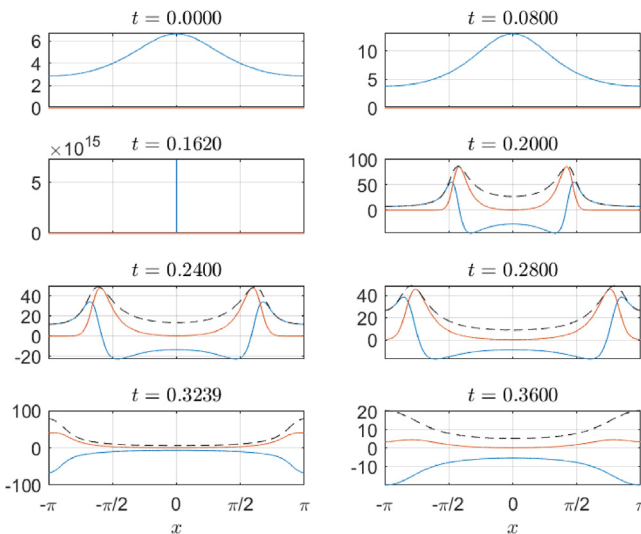


Fig. 9. Same as Fig. 8 but here the u -solution is shown. Note the blow up at $t = t_c$ and the near blow up at $t = 2t_c$. The dashed curve is the modulus $|u|$ (shown only after the first blow up). Note that the scales on the vertical axes are different in each frame.

into the initial condition.⁴ It was experiments based on these two ideas that lead us to the conjecture of four possible solutions after blow up, as shown in Fig. 10.

The same strategy worked for the related equations $u_t = u_{xx} + u^m$ (with m an integer greater than 2) and $u_t = u_{xx} + e^u$, both of which can be converted to more benign v -equations [11]. The results were qualitatively similar to those shown in Figs. 8–9. However, going from one space dimension to two poses a bigger computational challenge, one we have not yet taken up.

⁴ More specifically, we initialised the Fourier coefficients of the imaginary part at $t = 0$ with values taken randomly from a uniform distribution on $[-\epsilon, \epsilon]$, where ϵ is machine epsilon in MATLAB (approximately 2.2×10^{-16}).

One priority for future investigations is a better understanding of the transition from a real to a complex solution and the associated non-uniqueness. In our case the growth in the imaginary part is triggered, precisely at the critical time, by noise at the level of roundoff error. The randomness dictates whether the continuation is with one solution or another.

5. Conclusions

We investigated, asymptotically and numerically, point blow-up solutions to a periodic nonlinear heat Eq. (1) with nearly full initial data by considering the solution u in the reciprocal variable $v = 1/u$. We derived asymptotic approximations for the solution on the entire spatial interval and from $t = 0$ up to and including at the blow-up time, for which we also derived a second-order approximation. Due to the high accuracy of the Fourier spectral method (including at the blow-up time at which the v -solution has a weak singularity, unlike the u -solution), we were able to check numerically the validity of the asymptotics. We believe it is unusual for a single numerical method to confirm asymptotics in multiple regimes since typically numerical methods are weak, or highly inefficient, in most asymptotic limits unless they are highly specialised. The key to the success of the numerical method used here is the fact that it approximates the relatively well-behaved v -equation (3) rather than the u -equation (1) whose solution becomes unbounded. An additional and novel benefit of this numerical method is that it is able to compute post-blow-up solutions without requiring a deformation of the integration path into the complex-time plane.

The investigations in this paper point to a number of topics for future research, not least of which is the validity of the post-blow-up solutions computed in Section 4. In addition, the dynamics of complex singularities of blow-up solutions to (1) for a larger class of initial conditions, including initial data leading to non-generic forms of blow up, will be investigated in [18], also via a combination of asymptotic and numerical methods. In [18] we shall also explore the singularity structure of these blow-up solutions on their Riemann surfaces in the complex x -plane.

CRediT authorship contribution statement

M. Fasondini: Concept, Design, Analysis, Writing – review & editing. **J.R. King:** Concept, Design, Analysis, Writing – review & editing. **J.A.C. Weideman:** Concept, Design, Analysis, Writing – review & editing.

Declaration of competing interest

The authors declare that they have no known competing financial interests or personal relationships that could have appeared to influence the work reported in this paper.

Data availability

Data will be made available on request.

Acknowledgements

The first author is grateful to Saleh Tanveer for stimulating and insightful discussions. This research was started while the three authors were in residence at the Isaac Newton Institute for Mathematical Sciences as part of the programme *Complex analysis: techniques, applications and computations*. This programme was supported by: EPSRC, United Kingdom grant number EP/R014604/1. The work of the first author was also supported by the Leverhulme Trust Research Project Grant RPG-2019-144. The second author gratefully acknowledges a Leverhulme Trust Fellowship. A grant to the third author from the H.B. Thom foundation of Stellenbosch University is also gratefully acknowledged.

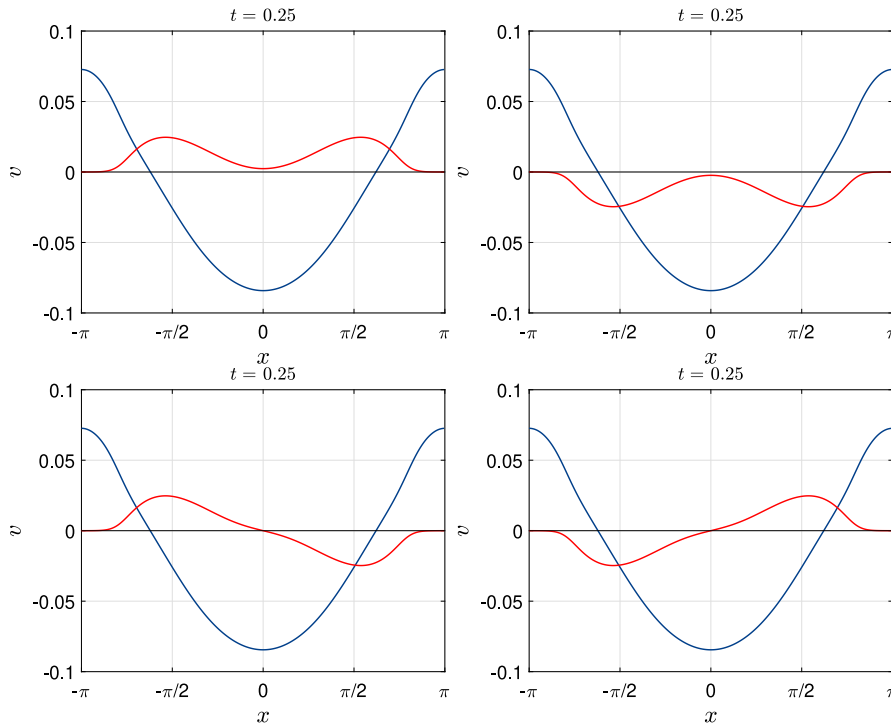


Fig. 10. Four conjectured solutions to (3) for the case $t > t_c$. The first frame represents the solution shown in Fig. 8, while the others are produced by experimentation with our numerical method as described in the text.

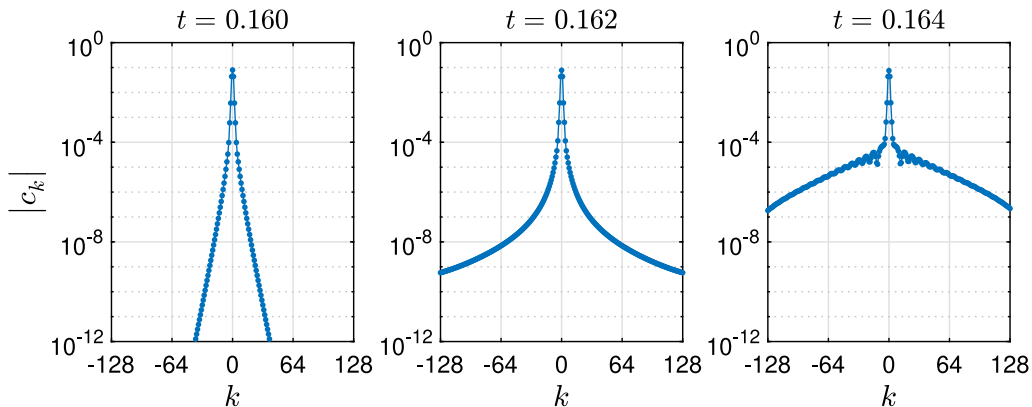


Fig. 11. Modulus of the Fourier coefficients c_k of the solution v shown in Fig. 8. The times are just prior to $t = t_c$, at $t = t_c$, and shortly after. (The value of t_c is given to more digits in Table 1.) In the first frame the coefficients decay exponentially, indicative of a function analytic in a neighbourhood of the real axis. At $t = t_c$ the coefficients decay algebraically as given by (25), because of the influence of the singularity of v as it reaches the origin. In the third frame the rate of decay in the coefficients is not immediately clear and warrants further investigation. However, the fact that the spectrum is no longer perfectly symmetric with respect to $k = 0$ indicates that the solution has turned complex..

Appendix A. Analysis via the method of matched asymptotic expansions

A.1. Truncated Fourier expansion

In this section we revisit and expand the analysis based on the two-mode Fourier truncation outlined in Section 2. Recall that by substituting (6) into the v -equation (3) and neglecting the $\cos 2x$ term the system (7) was obtained. From this, one finds by a self consistency argument⁵ that near blow-up, generically (i.e. even

⁵ $a = b$ at $t = t_c$ is required for $v = 0$ at $x = 0$; that is, generically a non-zero constant is confirmed by the expansions (26) that contain the requisite two degrees of freedom, namely a_c and t_c .

for $\epsilon = O(1)$)

$$a \sim a_c + (1 + 2a_c)(t_c - t), \quad b \sim a_c - a_c(t_c - t), \quad t \rightarrow t_c^-, \quad (26)$$

where a_c and the blow up time t_c are positive constants, so that the blow-up behaviour associated with (6) takes the form

$$v \sim (1 + 3a_c)(t_c - t) + \frac{1}{2}a_c x^2, \quad t \rightarrow t_c^-, \quad x = O((t_c - t)^{1/2}). \quad (27)$$

We emphasise that (26)–(27) describe the blow-up behaviour of (7) rather than that of (3): (27) has features in common with, but is not a valid representation of, the blow-up behaviour of the full PDE (3), a key point to which we shall return.

In keeping with our goal of characterising the behaviour of (3) for near-flat initial conditions, we now develop a fully analytic

asymptotic description of the behaviour of the two-mode system (7) for initial conditions (9) with $\alpha = O(1)$, $\epsilon \rightarrow 0^+$. There are two timescales; the first coincides with (10), so that at leading order (11) and (12) follow.

On the second time scale, and near blow up, we set

$$t = \alpha + \epsilon T, \quad b = \epsilon B, \quad a = \epsilon A_0(T) + O(\epsilon^2), \quad B = B_0(T) + O(\epsilon), \quad (28)$$

with $T = O(1)$, so that

$$\begin{aligned} A_0 \frac{dA_0}{dT} + \frac{1}{2} B_0 \frac{dB_0}{dT} &= -A_0, \\ B_0 \frac{dA_0}{dT} + A_0 \frac{dB_0}{dT} &= -B_0. \end{aligned} \quad (29)$$

Since $A_0 \pm \frac{1}{\sqrt{2}} B_0$ each satisfy

$$\Phi \frac{d\Phi}{dT} = -\Phi$$

we find on matching with (11)–(12) that

$$A_0 = -T, \quad B_0 = e^{-\alpha} \quad (30)$$

(a result that relies on the observation that a has no $O(\epsilon)$ contribution for $t = O(1)$, see (12)). Thus

$$t_c \sim \alpha - \epsilon e^{-\alpha}, \quad a_c \sim \epsilon e^{-\alpha}, \quad \epsilon \rightarrow 0^+$$

in (26)–(27). Moreover, while the rescaling (28) leads to a modified balance, i.e. (29) in place of (11) and (12), the result (30) implies that the solution passes unscathed through $T = O(1)$, with (11)–(12) being recovered for $t > \alpha$. Thus with the two-mode approximation (6) and (8) continuation through blow up seems to be straightforward, in contrast to that of the v -equation (3), as we shall subsequently demonstrate.

A.2. Truncated Taylor expansion

Much of what follows in this subsection revisits results from [11], which we derive using a different approach (namely, matched asymptotic expansions).

As in Section 2, we also consider the truncated Taylor approximation (5), which gives rise to the system (18) whose blow-up behaviour takes the form (again, by a self-consistency argument)

$$a \sim t_c - t, \quad b \sim \frac{1}{8(-\log(t_c - t) + b_c)}, \quad t \rightarrow t_c^- \quad (31)$$

for constants t_c and b_c . In contrast to the results of the previous subsection, (18) does capture the blow-up behaviour of the full PDE (3), a point to which we shall also come back.

We now return to initial conditions of the form (9), with the scalings (10) applying for $t = O(1)$, so expanding in the form

$$a \sim a_0 + \epsilon a_1, \quad b = \epsilon B, \quad B \sim B_0 + \epsilon B_1,$$

(18) implies

$$a_0 = \alpha - t, \quad B_0 = 1, \quad a_1 = 2t, \quad B_1 = 8 \log((\alpha - t)/\alpha). \quad (32)$$

Under the scalings (28) the leading-order balances do not change and the results of relevance below read

$$A_0 = 2\alpha - T, \quad B_0 = 1, \quad B_1 = 8 \log((2\alpha - T)/\alpha), \quad (33)$$

the matching into a_1 in (32) leading to the 2α contributions. The final scale in this case is then more subtle than those above: we set

$$a = (T_c - T)\hat{a}(\tau), \quad B = \hat{b}(\tau), \quad \tau = -\epsilon \log(T_c - T), \quad (34)$$

where

$$T_c \sim 2\alpha, \quad t_c \sim \alpha + 2\epsilon\alpha, \quad \epsilon \rightarrow 0^+. \quad (35)$$

The introduction of τ in (34) is associated with the expansion for B in (33) disordering and (18) becomes

$$\begin{aligned} \epsilon \frac{d\hat{a}}{d\tau} - \hat{a} &= 2\epsilon \hat{b} - 1, \\ \hat{a} \frac{d\hat{b}}{d\tau} &= -8\hat{b}^2, \end{aligned} \quad (36)$$

so that, on matching with (33),

$$\hat{a}_0 = 1, \quad \hat{b}_0 = \frac{1}{1 + 8\tau}, \quad \hat{a}_1 = -\frac{2}{1 + 8\tau}, \quad (37)$$

so that $b_c \sim 1/(8\epsilon)$ in (31).

For reasons that will become apparent below, it is instructive to record the implications of (37) under the scaling

$$x = \epsilon^{1/2} X \quad (38)$$

whereby

$$v \sim \epsilon \left(T_c - T + \frac{\epsilon}{1 + 8\tau} (X^2 - 2(T_c - T)) \right);$$

this will reappear in the analysis below in describing the local blow-up behaviour, but also confirms that (5) cannot describe the spatial profile at blow up (since at $T = T_c$ both terms in the ansatz (5) should vanish).

A.3. More general near-flat initial data

We now turn to the derivation of the blow-up behaviour, subjecting (3), the full PDE, to the initial data

$$v(x, 0) = \alpha + \epsilon V(x)$$

with, again, $0 < \epsilon \ll 1$. It is striking that this limit allows a near complete analytical description of the transition to blow up through the fully nonlinear regime. Three time scales are required. (I) On the first time scale:

$$t = O(1), \quad v \sim v_0(t) + \epsilon v_1(x, t) + \epsilon^2 v_2(x, t). \quad (I)$$

All three terms in this expansion are required for what follows. An immediate result is that

$$v_0 = \alpha - t$$

leading to

$$\frac{\partial v_1}{\partial t} = \frac{\partial^2 v_1}{\partial x^2}, \quad v_1(x, 0) = V(x). \quad (39)$$

We shall consider general $V(x)$, but in the case of real-valued 2π -periodic initial conditions (or zero Neumann boundary conditions on a finite domain⁶), we can Fourier decompose in the usual way, so that

$$v_1(x, t) = \sum_{k=-\infty}^{\infty} a_k e^{ikx - k^2 t}.$$

We note this special case for two reasons – firstly for its relevance to Appendix A.1 and secondly for the obvious observation that the high-frequency modes are rapidly decaying, providing additional motivation for the analysis of Sections 2 and A.1 but being also in some respects counter-intuitive, given that point blow up subsequently ensues.

⁶ This correspondence is worth emphasising with regard to the physical applicability and interpretation of the results.

We define

$$\Phi_1(x) = v_1(x, \alpha)$$

so that

$$v_1(x, t) \sim \Phi_1(x) - (\alpha - t)\Phi_1''(x), \quad t \rightarrow \alpha^- \tag{40}$$

At next order we have

$$\frac{\partial v_2}{\partial t} - \frac{\partial^2 v_2}{\partial x^2} = -\frac{2}{\alpha - t} \left(\frac{\partial v_1}{\partial x} \right)^2, \quad v_2(x, 0) = 0, \tag{41}$$

so that

$$v_2(x, t) \sim 2(\Phi_1'(x))^2 \log(\alpha - t) + \Phi_2(x) - 2 \left[(\Phi_1')^2 \right]'' (\alpha - t) \log(\alpha - t) + (4(\Phi_1'')^2 - \Phi_2'')(\alpha - t), \quad t \rightarrow \alpha^-, \tag{42}$$

where (42) serves to define $\Phi_2(x)$.

(II) On the second time scale:

$$T = O(1), \quad v = \epsilon w,$$

$$w \sim w_0(x, T) + \epsilon \log(1/\epsilon)w_1(x, T) + \epsilon w_2(x, T). \tag{II}$$

Here $t = t_c(\epsilon) + \epsilon T$, with $t_c(0) = \alpha$ and with correction terms to t_c identified below.⁷ We shall also need to consider the rescaling (38). We have

$$w \frac{\partial w}{\partial T} = \epsilon \left(w \frac{\partial^2 w}{\partial x^2} - 2 \left(\frac{\partial w}{\partial x} \right)^2 \right) - w$$

so, matching with (40), (42), and defining β_1 and β_2 via

$$t_c(\epsilon) \sim \alpha + \epsilon\beta_1 + \epsilon^2\beta_2, \quad \epsilon \rightarrow 0 \tag{43}$$

it follows for $x = O(1)$ that

$$w_0 = -T + \Phi_1(x) - \beta_1, \tag{44}$$

$$w_1 = -2(\Phi_1'(x))^2 \tag{45}$$

and hence

$$\frac{\partial w_2}{\partial T} = \Phi_1''(x) - \frac{2}{-T + \Phi_1(x) - \beta_1} (\Phi_1'(x))^2,$$

implying

$$w_2 = -(-T)\Phi_1''(x) + 2(\Phi_1'(x))^2 \log(-T + \Phi_1(x) - \beta_1) + \Phi_2(x) - \beta_2. \tag{46}$$

We take blow up to occur at $x = 0$, requiring that $\Phi_1'(0) = \Phi_2'(0) = 0$ and take

$$\Phi_1(x) \sim \beta_1 + \gamma_1 x^2, \quad \Phi_2(x) \sim \beta_2 + \gamma_2 x^2, \quad x \rightarrow 0 \tag{47}$$

for constants $\beta_{1,2}, \gamma_{1,2}$ with $\gamma_1 > 0$,⁸ and where the requirement that $w = 0$ at $x = 0, T = 0$ implies that $\beta_{1,2}$ in (43) are specified by (47) with $\Phi_{1,2}$ being determined by the linear problems (39) and (41).

For $X = O(1)$ (see (38)), we first generate the required matching conditions from (40), (42) and (47), whereby

$$w \sim -T + (\epsilon\gamma_1 - 8\epsilon^2 \log(1/\epsilon)\gamma_1^2 + 8\epsilon^2\gamma_1^2 \log(-T) + \epsilon^2\gamma_2)(X^2 - 2(-T)) + 16\epsilon^2\gamma_1^2(-T), \tag{48}$$

wherein we have retained only the required terms in X^0 and X^2 – in general v_1 will also lead to contributions of the form

$$\epsilon^{3/2}(X^3 - 6(-T)X), \quad \epsilon^2(X^4 - 12(-T)X^2 + 12(-T)^2)$$

in w but these can be neglected for our purposes, being subdominant as $T \rightarrow 0^-$ with $X = O((-T)^{1/2})$.

We have

$$w \frac{\partial w}{\partial T} = w \frac{\partial^2 w}{\partial X^2} - 2 \left(\frac{\partial w}{\partial X} \right)^2 - w \tag{49}$$

and from this we find that the relevant terms for $T = O(1)$ simply reproduce the matching condition (48) obtained from the expansion for $t = O(1)$. Importantly, the expansion (48) disorders for $\epsilon \log(-T) = O(1)$, as in Appendix A.2, leading us on to our third and final time scale, as follows. (III) On this exponentially short timescale⁹ with $\tau = -\epsilon \log((t_c - t)/\epsilon)$ the scalings are:

$$\tau = O(1), \quad w = (-T)g,$$

$$g \sim 1 + \epsilon g_1(\xi, \tau) + \epsilon^2 \log(1/\epsilon)g_2(\xi, \tau) + \epsilon^2 g_3(\xi, \tau) \tag{III}$$

where

$$\xi = \frac{X}{(-T)^{1/2}}. \tag{50}$$

We emphasise that much of what follows reconstructs known blow-up behaviour (see the review of [16], for example.) The novelty here lies in the focus on the near-flat initial data, which allows a significantly more detailed characterisation of the full spatial behaviour.

The near self-similar solution ansatz (50) transforms (49) to

$$\epsilon g \frac{\partial g}{\partial \tau} - g^2 + \frac{1}{2} \xi g \frac{\partial g}{\partial \xi} = g \frac{\partial^2 g}{\partial \xi^2} - 2 \left(\frac{\partial g}{\partial \xi} \right)^2 - g$$

so that

$$-g_1 + \frac{1}{2} \xi \frac{\partial g_1}{\partial \xi} = \frac{\partial^2 g_1}{\partial \xi^2}, \tag{51}$$

implying that

$$g_1 = \sigma_1(\tau)(\xi^2 - 2); \tag{52}$$

similarly

$$g_2 = \sigma_2(\tau)(\xi^2 - 2) \tag{53}$$

but g_3 satisfies (following cancellation of a number of terms using (51))

$$\frac{d\sigma_1}{d\tau}(\xi^2 - 2) - g_3 + \frac{1}{2} \xi \frac{dg_3}{d\xi} = \frac{d^2 g_3}{d\xi^2} - 8\sigma_1^2 \xi^2. \tag{54}$$

Since we need to preclude exponential growth of g_3 (i.e. to exclude contributions with $\log g_3 \sim \xi^2/4$ as $\xi \rightarrow \pm\infty$), (54) both requires that

$$g_3 = -2 \frac{d\sigma_1}{d\tau} + \sigma_3(\tau)(\xi^2 - 2) \tag{55}$$

and generates the solvability condition

$$\frac{d\sigma_1}{d\tau} = -8\sigma_1^2; \tag{56}$$

that the $O(\epsilon)$ term in g is only fully determined via (54) necessitates that the expansion be taken up to $O(\epsilon^2)$. Matching with (48) then requires that

$$\sigma_1 = \frac{\gamma_1}{1 + 8\gamma_1\tau}, \quad -2 \frac{d\sigma_1}{d\tau} = \frac{16\gamma_1^2}{(1 + 8\gamma_1\tau)^2}, \tag{57}$$

⁷ The notation here differs somewhat from that of the previous subsections.

⁸ The case $\gamma_1 = 0$ corresponds to non-generic forms of blow up – we shall not pursue such matters here.

⁹ This feature makes the behaviour on this timescale exceptionally hard to capture numerically, illustrating the well-known complementarity between asymptotic and numerical approaches.

simultaneously confirming matching with the second, fourth and final terms in (48). The calculation of σ_2 and σ_3 requires solvability conditions at yet higher orders (which we will not pursue), with (48) requiring that

$$\sigma_2(0) = -8\gamma_1^2, \quad \sigma_3(0) = \gamma_2.$$

By analogy with the subdivision into x and X in (II), we need also to consider $\eta = O(1)$, where

$$\eta = \frac{x}{(-T)^{1/2}}, \quad \eta = \epsilon^{1/2}\xi,$$

though a third scale (namely $x = O(1)$) will also require consideration here. Since

$$\epsilon g \frac{\partial g}{\partial \tau} - g^2 + \frac{1}{2} \eta g \frac{\partial g}{\partial \eta} = \epsilon \left(g \frac{\partial^2 g}{\partial \eta^2} - 2 \left(\frac{\partial g}{\partial \eta} \right)^2 \right) - g,$$

setting

$$g \sim G_0(\eta, \tau) + \epsilon \log(1/\epsilon) G_1(\eta, \tau) + \epsilon G_2(\eta, \tau)$$

gives on matching into $\xi = O(1)$

$$G_0 = 1 + \sigma_1(\tau)\eta^2, \quad G_1 = \sigma_2(\tau)\eta^2 \tag{58}$$

and

$$\frac{1}{2} \eta \frac{dG_2}{d\eta} - G_2 = 2\sigma_1 - \frac{d\sigma_1}{d\tau} \eta^2 - \frac{8\sigma_1^2 \eta^2}{1 + \sigma_1 \eta^2},$$

so that, again matching into $\xi = O(1)$,

$$G_2 = -2\sigma_1(\tau) + 8\sigma_1^2(\tau)\eta^2 \log(1 + \sigma_1(\tau)\eta^2) + \sigma_3(\tau)\eta^2; \tag{59}$$

were σ_1 not a solution to (56), a term in $\log \eta$ would also be present here, further clarifying the status of (56) as a solvability condition.

Finally, we can simply set $T = 0$ in (44)–(46), noting that $\tau = O(1)$ corresponds to exponentially small T , to obtain the profile at blow up for $x = O(1)$.¹⁰ Thus as $t \rightarrow t_c^-$, $\epsilon \rightarrow 0$ with $x = O(1)$ we have

$$w \sim \Phi_1(x) - \beta_1 - 2\epsilon \log(1/\epsilon) (\Phi_1'(x))^2 + \epsilon \left(2 (\Phi_1'(x))^2 \log(\Phi_1(x) - \beta_1) + \Phi_2(x) - \beta_2 \right). \tag{60}$$

The expression (60) has small- x behaviour

$$w \sim \gamma_1 x^2 - 8\epsilon \log(1/\epsilon) \gamma_1^2 x^2 + \epsilon (8\gamma_1^2 x^2 \log(\gamma_1 x^2) + \gamma_2 x^2), \tag{61}$$

The expressions (60)–(61) do not apply for exponentially small x , however. Instead, we need to extract from (58)–(59) the terms relevant for large η , namely

$$g \sim \sigma_1 \eta^2 + 16\epsilon \sigma_1^2 \eta^2 \log \eta,$$

these being of the same order for $\epsilon \log \eta = O(1)$.

Reconstructing w from these using (57), we have

$$w \sim \frac{\gamma_1}{1 + 8\gamma_1 \tau} x^2 + \frac{16\epsilon \gamma_1^2 x^2}{(1 + 8\gamma_1 \tau)^2} \log \eta,$$

which, using

$$\tau = -2\epsilon \log x + 2\epsilon \log \eta,$$

implies that

$$w \sim \frac{\gamma_1 x^2}{1 - 16\epsilon \gamma_1 \log |x|} \tag{62}$$

¹⁰ The evolution on the third timescale affects the exponentially small lengthscales $x = O((-T)^{1/2})$ and $X = O((-t)^{1/2})$, the behaviour for $x = O(1)$ being retained from (II).

describes the profile at blow up for x exponentially small with respect to ϵ (having taken the various limits in the appropriate order); (62) matches with the relevant terms in (61) for larger x .

We note that non-analytic (i.e. logarithmic) terms here occur as a matter of course, in $(t_c - t)$ in (57) and in x in (61): these arise constructively in the current analysis rather than being introduced a priori as part of a solution ansatz. That the current limit provides a detailed asymptotic characterisation of the profile (60) at blow up for almost all x , not just close to blow-up point, is also noteworthy.

A.3.1. Comparison with truncated expansions

The above systematic asymptotic analysis clarifies the extent of applicability of the ad-hoc approximations treated in Appendices A.1 and A.2.

Starting with a comparison with the results of Appendix A.2, we have already noted that the truncated Taylor expansion correctly captures the blow-up behaviour, as can be substantiated by the following observations. For $V(x) = x^2$ it follows that

$$\begin{aligned} v_1 &= x^2 + 2t, \\ v_2 &= 8x^2 \log((\alpha - t)/\alpha) - 16(\alpha - t) \log((\alpha - t)/\alpha) - 16t, \\ \Phi_1 &= x^2 + 2\alpha, \quad \Phi_2 = -8x^2 \log \alpha - 16\alpha, \end{aligned} \tag{63}$$

which imply (see (43) and (47))

$$\begin{aligned} \beta_1 &= 2\alpha, \quad \gamma_1 = 1, \quad \beta_2 = -16\alpha, \\ \gamma_2 &= -8 \log \alpha, \quad t_c \sim \alpha + 2\alpha\epsilon - 16\alpha\epsilon^2. \end{aligned} \tag{64}$$

More importantly, (48), (52), (53), (55) and (58) are all quadratic in x for general $V(x)$, so the approximation in Appendix A.2 represents an attractor in that sense. As already noted, it cannot capture the spatial blow-up profile, the first manifestation of this being represented by the logarithmic term in (59); see also (61) and (62). It is especially noteworthy that (55) is a quadratic in ξ ; if the corresponding analysis is undertaken on (1) rather than on (3), a ξ^4 term arises at that order. This represents a hidden benefit of the v formulation.

Turning now to Appendix A.1, corresponding to $V(x) = -\cos x$, we can both exemplify the form of the profile (60) at blow up and indicate where the analysis of Appendix A.1 breaks down in describing the behaviour of the full PDE. In this case

$$\begin{aligned} v_1 &= -e^{-t} \cos x, \\ v_2 &= -\int_0^t \frac{e^{-2s}}{\alpha - s} ds - e^{-4t} \int_0^t \frac{e^{2s}}{\alpha - s} ds \cos(2x), \\ \Phi_1 &= -e^{-\alpha} \cos x, \quad \Phi_2 = -C_1 - C_2 - (C_1 + C_3) \cos 2x, \end{aligned} \tag{65}$$

where

$$\begin{aligned} C_1 &= e^{-2\alpha} \log \alpha, \quad C_2 = \int_0^\alpha \frac{e^{-2t} - e^{-2\alpha}}{\alpha - t} dt, \\ C_3 &= e^{-4\alpha} \int_0^\alpha \frac{e^{2t} - e^{2\alpha}}{\alpha - t} dt, \end{aligned} \tag{66}$$

which imply (see (47))

$$\begin{aligned} \beta_1 &= -e^{-\alpha}, \quad \gamma_1 = \frac{e^{-\alpha}}{2}, \\ \beta_2 &= -2C_1 - C_2 - C_3, \quad \gamma_2 = 2(C_1 + C_3). \end{aligned} \tag{67}$$

That v_2 and Φ_2 contain $\cos 2x$ contributions is already indicative of the failure of the truncated Fourier expansion close to the blow up; nevertheless, v_1 and w_0 (in (44)) provide the dominant spatial dependencies on the relevant scales and retain the form of Appendix A.1 (and the $O(\epsilon)$ term in (48) can be viewed as

being associated with the latter's Taylor expansion). The truncation is, however, entirely unable to reproduce the behaviour for $\tau = O(1)$, manifesting nothing reflecting the solvability argument leading to (56).

Notwithstanding their deficiencies, the simple approximations of Appendices A.1 and A.2 are instructive both for familiar reasons (namely for the transparency and simplicity of their analysis) and because they can immediately be analytically continued to assess their relevance to the evolution of singularities in the complex plane; see Fig. 4 (in which the dashed line is derived from the approximation of Appendix A.1).

A.4. Complex-singularity dynamics

The motion of the singularity necessarily breaks down into the three time scales of Appendix A.3 (labelled (I), (II) and (III)) and here we adopt the specific initial condition $v = \alpha - \epsilon \cos x$. We set $x = iy$ and describe the location of the nearest singularity (corresponding to $v = 0$) on the positive imaginary axis.

On the first time scale ($t = O(1)$), we set $y = \log(1/\epsilon) + Y$ in (3) and have the full balance

$$v \frac{\partial v}{\partial t} = - \left(v \frac{\partial^2 v}{\partial Y^2} - 2 \left(\frac{\partial v}{\partial Y} \right)^2 \right) - v, \tag{68}$$

now to be solved as an initial value problem subject to

$$\text{at } t = 0, \quad v = \alpha - \frac{1}{2} e^Y, \tag{69}$$

$$\text{as } Y \rightarrow -\infty, \quad v \sim \alpha - t - \frac{1}{2} e^{Y-t}. \tag{70}$$

This not analytically solvable (and in effect a more difficult problem than the original PDE with nearly flat initial data), but does establish that to leading order the singularity location is fixed: $y \sim \log(1/\epsilon)$. This problem can, however, be solved analytically in the limits $t \rightarrow 0^+$ and $t \rightarrow \alpha^-$; using the techniques of [18], we find

$$y \sim \log(2\alpha/\epsilon) + (2t \log(1/t))^{1/2}, \quad t \rightarrow 0^+, \tag{71}$$

$$y \sim \log(2/\epsilon) + \alpha + \log(\alpha - t), \quad t \rightarrow \alpha^-, \tag{72}$$

so the singularity moves away from the real axis at early times (with unbounded speed as $t \rightarrow 0^+$) before reversing.

The results on the second and final time scales follow immediately from the above real line results. On the second time scale ($t = t_c + \epsilon T$, $T = O(1)$), since (see (44) and (65)–(67))

$$w_0 = -T - e^{-\alpha} (\cosh y - 1)$$

the singularity location satisfies

$$\cosh y \sim 1 + e^\alpha(-T) \tag{73}$$

so that

$$y \sim \log \left(1 + e^\alpha(-T) + (2e^\alpha(-T) + e^{2\alpha}(-T)^2)^{1/2} \right). \tag{74}$$

It follows from (74) that

$$y \sim \log(-2T) + \alpha, \quad T \rightarrow -\infty, \tag{75}$$

$$y \sim (2e^\alpha(-T))^{1/2}, \quad T \rightarrow 0^-, \tag{76}$$

where (75) exhibits the necessary matching with (72).

On the final time scale ($\tau = -\epsilon \log(-T)$, $\tau = O(1)$), since (see (58))

$$G_0 = 1 - \sigma_1 y^2 / (-T), \quad \sigma_1 = \frac{\gamma_1}{1 + 8\gamma_1 \tau},$$

with $\gamma_1 = 1/(2e^\alpha)$ the singularity location satisfies

$$y \sim (2e^\alpha(-T))^{1/2} (1 - 4\epsilon e^{-\alpha} \log(-T))^{1/2}, \tag{77}$$

which matches with (76) for $\epsilon |\log(-T)| \ll 1$, while

$$y \sim (8(t_c - t) \log(1/(t_c - t)))^{1/2}, \quad t \rightarrow t_c^-,$$

accordingly describes impingement onto the real axis.

Appendix B. Flatness of the solution on the real line and proximity of the nearest singularity

Note from Fig. 1 that the solutions to the u -equation (1) that we consider attain their maximum at $x = 0$ and their minimum at $x = \pm\pi$. Therefore, as an indication of the ‘flatness’ of the solution profile, we consider the quantity $u(0, t) - u(\pi, t) := f(t)$, which is the relative height of the peak of the solution on $[-\pi, \pi]$. We shall consider the relation between the flatness of the solution profile and the distance of the singularities to the real axis.

Let the $a_k(t)$ denote the Fourier coefficients of the solution in the u variable. Since the solution is real (prior to blow up) and even, $a_k = a_{-k}$ and thus the flatness of the solution is given by

$$f(t) = \sum_{k=-\infty}^{\infty} a_k(t) - \sum_{k=-\infty}^{\infty} (-1)^k a_k(t) = 4 \sum_{k=0}^{\infty} a_{2k+1}(t). \tag{78}$$

If $f' < 0$, the solution becomes more flat while if $f' > 0$ the solution becomes steeper on $x \in [-\pi, \pi]$. Using the residue theorem, it follows that

$$\begin{aligned} a_k(0) &= \frac{1}{2\pi} \int_{-\pi}^{\pi} \frac{e^{-ikx}}{\alpha - \epsilon \cos x} dx \\ &= \frac{\left(\frac{\alpha}{\epsilon} + \sqrt{\left(\frac{\alpha}{\epsilon} \right)^2 - 1} \right)^{-|k|}}{\epsilon \sqrt{\left(\frac{\alpha}{\epsilon} \right)^2 - 1}} \\ &= \frac{1}{\alpha} \left(\frac{\epsilon}{2\alpha} \right)^{|k|} + O(\epsilon^{|k|+2}), \quad \epsilon \rightarrow 0. \end{aligned} \tag{79}$$

The coefficients satisfy

$$a'_k = -k^2 a_k + b_k, \tag{80}$$

where b_k is the k th Fourier coefficient of u^2 .

It follows from (79)–(80) that, to leading order, as $\epsilon \rightarrow 0$, and away from the blow-up time,

$$a_0(t) \sim \frac{1}{\alpha - t}, \quad a_1(t) \sim \frac{\epsilon e^{-t}}{2(\alpha - t)^2}, \tag{81}$$

therefore

$$f'(t) \sim 4a'_1 \sim \frac{2\epsilon e^{-t}(t - (\alpha - 2))}{(\alpha - t)^3}.$$

Hence, on the real line, the solution switches from flattening to steepening at $t \sim \alpha - 2$ if $\alpha > 2$ and the minimal flatness is $f(\alpha - 2) \sim 4a_1(\alpha - 2) \sim \epsilon e^{2-\alpha}/2$. If $\alpha < 2$, the solution does not flatten at all but steepens from $t = 0$ until the blow-up time. Fig. 12 confirms the validity of the flatness approximation $f(t) \sim 4a_1(t)$ away from the blow-up time.

In the complex plane, we deduce from the asymptotic approximation (71) that, regardless of the parameter values (provided $\alpha \ll \epsilon$), the singularities initially move away from the real axis and turn around at $t \sim \exp(-1) \approx 0.37$, which is consistent with the numerical results in Fig. 4. This illustrates that there is not a simple correspondence between the distance of the singularity from the real axis and the flatness of the solution.

Indeed, it follows from (78) and the rapid decay of the Fourier coefficients (away from the blow-up time) that the flatness of the solution is determined by the behaviour of the low-order Fourier coefficient a_1 . On the other hand, the distance of the singularity from the real axis is determined by the behaviour of the high-order Fourier modes. Hence, the discrepancy between the flatness

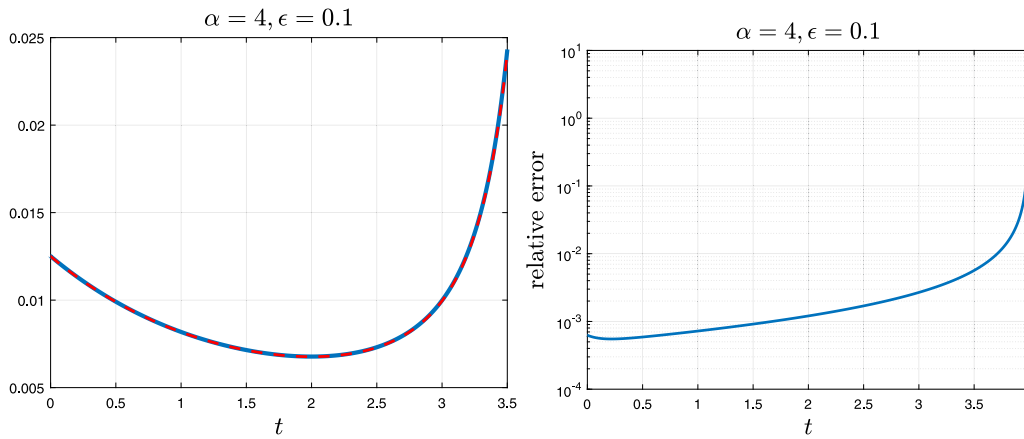


Fig. 12. Left: The numerically computed flatness $f(t) = u(0, t) - u(\pi, t)$ (solid blue curve) compared to the approximation $f(t) \sim 4a_1$, with a_1 given in (81) (red dashed curve). Right: the relative error of the approximation $f(t) \sim 4a_1$, which, as expected, ceases to be valid as blow up is approached.

of the solution and the proximity of the singularity is due to the qualitatively different evolution of the lower and higher order Fourier modes.

For the high-order modes, the diffusion term $-k^2 a_k$ dominates the nonlinear term b_k for small t (again, due to the rapid decay of the Fourier coefficients). Therefore $a'_k < 0$, the high-order Fourier coefficients decay for small t and therefore the singularity initially moves away from the real axis, regardless of the parameter values satisfying $\epsilon \ll \alpha$. The high-order Fourier coefficients start increasing as the singularity turns around, which occurs at $t \sim 0.37$, according to (71).

Appendix C. Asymptotic estimate of truncation error

Here we estimate the error that results from truncating the Fourier series (4) at $|k| = N$ in the numerical method.

Since for $t \in [0, t_c]$, the Fourier coefficients decay at their slowest rate at $t = t_c$, we can use the approximation (23) (whose accuracy is examined in right frame of Fig. 6) to estimate an upper bound on the spatial truncation error that is valid for $t \in [0, t_c]$. Ignoring the error incurred by the time integration method (whose tolerance we set to 10^{-12} , which we assume is negligible compared to the truncation error) and using the fact that the solution is even for $t \in [0, t_c]$, we estimate the squared 2-norm absolute truncation error to be

$$\left\| v(x, t) - \sum_{k=-N}^N c_k(t) e^{ikx} \right\|_2^2 \approx 2 \sum_{k=N+1}^{\infty} |c_k(t)|^2$$

Using (23), we have for $t \rightarrow t_c, \epsilon \rightarrow 0$ and $N \rightarrow \infty$ that

$$2 \sum_{k=N+1}^{\infty} |c_k(t)|^2 \sim 32\epsilon^4 e^{-4\alpha} \sum_{k=N+1}^{\infty} k^{-6} \sim \frac{32\epsilon^4 e^{-4\alpha}}{5N^5}.$$

It follows from (22) that as $t \rightarrow t_c$ and $\epsilon \rightarrow 0$

$$\|v(x, t)\|_2^2 \sim 4\epsilon^2 e^{-2\alpha} \int_{-\pi}^{\pi} \sin^4(x/2) dx = 3\pi\epsilon^2 e^{-2\alpha}.$$

Hence, in the limits given above we estimate the relative spatial truncation error to be

$$4\sqrt{\frac{2}{15\pi}} \frac{\epsilon e^{-\alpha}}{N^{5/2}}. \tag{82}$$

For the numerical experiments reported in this paper we set $N = 128$, in which case the error estimate is $C\epsilon e^{-\alpha}$ with $C = 4.45 \times 10^{-6}$.

Appendix D. Supplementary data

Supplementary material related to this article can be found online at <https://doi.org/10.1016/j.physd.2023.133660>.

References

- [1] S. Braun, A. Kluwick, Unsteady three-dimensional marginal separation caused by surface-mounted obstacles and/or local suction, *J. Fluid Mech.* 514 (2004) 121–152.
- [2] S. Braun, A. Kluwick, Blow-up and control of marginally separated boundary layers, *Philos. Trans. R. Soc. Lond. Ser. A Math. Phys. Eng. Sci.* 363 (1830) (2005) 1057–1067.
- [3] L.M. Hocking, K. Stewartson, J.T. Stuart, S.N. Brown, A nonlinear instability burst in plane parallel flow, *J. Fluid Mech.* 51 (4) (1972) 705–735.
- [4] J.W. Dold, On asymptotic forms of reactive-diffusive runaway, *Proc. R. Soc. Lond. Ser. A Math. Phys. Eng. Sci.* 433 (1889) (1991) 521–545.
- [5] M.A. Herrero, J.J.L. Velázquez, Plane structures in thermal runaway, *Israel J. Math.* 81 (3) (1993) 321–341.
- [6] A.A. Lacey, Mathematical analysis of thermal runaway for spatially inhomogeneous reactions, *SIAM J. Appl. Math.* 43 (6) (1983) 1350–1366.
- [7] S. Jabbari, J.R. King, Discrete and continuum multiscale behaviour in bacterial communication, in: *Multiscale Computer Modeling in Biomechanics and Biomedical Engineering*, Springer, 2013, pp. 299–320.
- [8] D.M. Ambrose, P.M. Lushnikov, M. Siegel, D.A. Silant'ev, Global existence and singularity formation for the generalized Constantin–Lax–Majda equation with dissipation: The real line vs. periodic domains, 2022, <https://arxiv.org/abs/2207.07548>.
- [9] M. Berger, R.V. Kohn, A rescaling algorithm for the numerical calculation of blowing-up solutions, *Comm. Pure Appl. Math.* 41 (6) (1988) 841–863.
- [10] C.J. Budd, Jianping Chen, W. Huang, R.D. Russell, Moving mesh methods with applications to blow-up problems for PDEs, in: *Numerical Analysis 1995*, Dundee, 1995, in: *Pitman Res. Notes Math. Ser.*, vol. 344, Longman, Harlow, 1996, pp. 1–18.
- [11] J.B. Keller, J.S. Lowengrub, Asymptotic and numerical results for blowing-up solutions to semilinear heat equations, in: *Singularities in Fluids, Plasmas and Optics*, Heraklion, 1992, in: *NATO Adv. Sci. Inst. Ser. C Math. Phys. Sci.*, vol. 404, Kluwer Acad. Publ., Dordrecht, 1993, pp. 111–129.
- [12] C. Sulem, P.L. Sulem, H. Frisch, Tracing complex singularities with spectral methods, *J. Comput. Phys.* 50 (1) (1983) 138–161.
- [13] Y. Tourigny, M. Grinfeld, Deciphering singularities by discrete methods, *Math. Comp.* 62 (205) (1994) 155–169.
- [14] J.A.C. Weideman, Computing the dynamics of complex singularities of nonlinear PDEs, *SIAM J. Appl. Dyn. Syst.* 2 (2003) 171–186.
- [15] S. Dejak, Z. Gang, I.M. Sigal, S. Wang, Blow-up in nonlinear heat equations, *Adv. Appl. Math.* 40 (4) (2008) 433–481.
- [16] V.A. Galaktionov, J.L. Vázquez, The problem of blow-up in nonlinear parabolic equations, *Discrete Contin. Dyn. Syst.* 8 (2) (2002) 399–433.

- [17] P. Quittner, P. Souplet, *Superlinear Parabolic Problems: Blow-Up, Global Existence and Steady States*, Springer, 2019.
- [18] M. Fasandini, J. King, J.A.C. Weideman, *Complex-plane singularity dynamics for blow up in a nonlinear heat equation: analysis and computation*, 2023 in preparation.
- [19] L.F. Shampine, M.W. Reichelt, *The MATLAB ODE suite*, *SIAM J. Sci. Comput.* 18 (1) (1997) 1–22.
- [20] K. Masuda, *Analytic solutions of some nonlinear diffusion equations*, *Math. Z.* 187 (1) (1984) 61–73.
- [21] C.-H. Cho, H. Okamoto, M. Shoji, *A blow-up problem for a nonlinear heat equation in the complex plane of time*, *Jpn. J. Ind. Appl. Math.* 33 (1) (2016) 145–166.
- [22] A. Takayasu, J.P. Lessard, J. Jaquette, H. Okamoto, *Rigorous numerics for nonlinear heat equations in the complex plane of time*, *Numer. Math.* 151 (3) (2022) 693–750.